Li and Na Diffusion in TiO_2 from Quantum Chemical Theory versus Electrochemical Experiment

Sten Lunell,*,† Arvids Stashans,† Lars Ojamäe,‡ Henrik Lindström,§ and Anders Hagfeldt§

Contribution from the Department of Quantum Chemistry, Uppsala University, Box 518, S-751 20 Uppsala, Sweden, Department of Physical, Inorganic and Structural Chemistry, Arrhenius Laboratory, Stockholm University, S-106 91 Stockholm, Sweden, and Department of Physical Chemistry, Uppsala University, Box 532, S-751 21 Uppsala, Sweden

Received March 17, 1997. Revised Manuscript Received June 3, 1997[⊗]

Abstract: Diffusion of Li and Na ions in TiO_2, anatase, has been studied using theoretical (quantum chemical *ab initio* periodic Hartree−Fock and a modified semiempirical INDO) as well as electrochemical (chronocoloumetry) methods. On the basis of the theoretical calculations, the geometry of equilibrium and transition states for the impurities as well as the crystalline framework are analyzed and discussed. The calculated activation energies for Li^+ and Na^+ diffusion were found to be only slightly higher than 0.5 eV by both theoretical methods. The agreement of either theoretical method with the electrochemical experiments, 0.60 and 0.52 eV for Li^+ and Na^+, respectively, is also remarkably good.

Introduction

Cation intercalation in titanium dioxide has been studied extensively, in particular for its electrochromic[1] and charge storage (secondary batteries)[2] properties. In general, the uptake of, for example, Li^+ has been found to be much better in the anatase lattice compared to the rutile structure.[3] The anatase structure has tetragonal symmetry, and the structure comprises TiO_6 octahedra sharing two adjacent edges with two other octahedra so that infinite planar double chains are formed. Vacant interstitial sites are large enough to accommodate H^+ and Li,$^+$ whereas other ions may be too large to fit into the crystal lattice. However, to our knowledge, only few studies are concerned with Na^+ and K^+ intercalation. For example, Kavan *et al.*[4] interpreted current−potential curves (cyclic voltammetry) for TiO_2 anatase electrodes immersed in a Na^+-containing electrolyte as due to capacitive currents, i.e., intercalation of sodium ions was considered not to be possible in the crystal lattice. A study by Strømme Mattsson *et al.*[5] discussed, on the other hand, mobilities of Na^+ in amorphous fluorinated Ti oxide films. Li and Na intercalation was suggested to progress without major structural changes. The chemical diffusion coefficients obtained from impedance spectroscopy, using a simple Randles circuit with a finite Warburg diffusion element, were found to be thermally activated with activation energies of around 0.5 and 1.6 eV for Li^+ and Na^+, respectively. However, theoretical computations using the INDO method, carried out in the same work,[5] suggested activation energies to be around 0.5 eV for both Li and Na ions in TiO_2 anatase, in agreement with experiment for Li but in serious disagreement for Na. In order to resolve this problem we have expanded our previous theoretical study by including another theoretical method, based on the *ab initio* technique, and also performed new electrochemical measurements based on chronocoloumetry.

The *ab initio* and semiempirical methods used in the present study are developed especially for crystal studies, i.e., calculations of total energy and electronic band structure of infinite periodic systems. These theoretical approaches are different, not only due to the non- and semiempirical backgrounds but also because of the way the total energy is calculated, as well as in their methods of geometry optimization. The theory is supported by new experiments, where the activation energies for Li^+ and Na^+ were determined electrochemically by measuring the diffusion coefficients at different temperatures. Chronocoloumetry was used because of the simplicity of this method.

Theoretical Method

***Ab Initio* Periodic Hartree−Fock Calculations.** The structures of the alkali-doped crystal and the ion diffusion path were investigated by means of the *ab initio* quantum-chemical program *Crystal95*.[6] Using this program it is possible to treat not only molecules or clusters but, in particular, crystalline solids at an *ab initio* level of theory, since the Hartree−Fock one-electron eq are solved subject to periodic boundary conditions.[7]

Whereas semiempirical and density-functional methods early on were applied to the solid state, especially in the discipline of solid state physics, *ab initio* calculations were not applied in a larger scale until the late 1980s and increasingly in the 1990s. Some examples include Al_2O_3,[8] Li_2O, Na_2O and K_2O,[9] $LiOH{\cdot}H_2O$,[10] the TiO_2 rutile[11,12] and anatase[13] phases, C-doped Si,[14] Li-doped NiO,[15] and bulk WO_3.[16]

† Department of Quantum Chemistry.
‡ Department of Physical, Inorganic and Structural Chemistry.
§ Department of Physical Chemistry.
⊗ Abstract published in *Advance ACS Abstracts,* July 15, 1997.

(1) Granqvist, C.-G. *Handbook of Inorganic Electrochromic Materials*; Elsevier: Amsterdam, 1995.
(2) Huang, S. Y.; Kavan, L.; Exnar, I.; Grätzel, M. *J. Electrochem. Soc.* **1995**, *142*, 142.
(3) Stashans, A.; Lunell, S.; Bergström, R.; Hagfeldt, A.; Lindquist, S.-E.; *Phys. Rev. B* **1996**, *53*, 159.
(4) Kavan, L.; Kratochilova, K.; Grätzel, M. *J. Electroanal. Chem.* **1995**, *394*, 93.
(5) Strømme Mattsson, M.; Veszelei, M.; Niklasson, G. A.; Granqvist, C.-G.; Stashans, A.; Lunell, S. In *Electrochromic Materials and Their Applications III*, Ho, K. C., Greenberg, C. B., MacArthur, D. M., Eds.; The Electrochem. Soc. Proc. Series PV 96-24, in press.
(6) Dovesi, R.; Saunders, V. R.; Roetti, C.; Causà, M.; Harrison, N. M.; Orlando, R.; Aprà, E. *Installation Manual 1.0, Nov.22, 1996*; Theoretical Chemistry Group, University of Turin (Italy), CCLRC Daresbury Laboratory (UK).
(7) Pisani, C.; Dovesi, R.; Roetti, C. *Ab Initio Treatment of Crystalline Solids, Lecture Notes in Chemistry 48*; Springer: Berlin, 1988.
(8) Salasco, L.; Dovesi, R.; Orlando, R.; Causà, M.; Saunders, V. R. *Mol. Phys.* **1991**, *72*, 267.
(9) Dovesi, R.; Roetti, C.; Freyria-Fava, C.; Prencipe, M.; Saunders, V. R. *Chem. Phys.* **1991**, *156*, 11.

S0002-7863(97)00862-7 CCC: $14.00

The basis set used consisted of atom-centred gaussian-type functions. For Ti and O, the basis set used was the set utilized by Fahmi *et al.*[13] For Ti, this consists of d-functions contracted to a (4/1) basis set plus a shell of sp polarization functions. The inner electrons were represented by an effective core potential (ECP) as derived by Durand and Barthelat.[17] For O the basis set was an ECP-31G set.[18] The Li and Na basis sets used were the ones developed by Dovesi *et al.*[9] for Li_2O and Na_2O crystals, but with the inner shells replaced by Durand−Barthelat effective core potentials. That basis consisted of a valence sp shell for Li and a valence plus a polarization *sp* shell for Na. In the present study, an sp shell with exponent 0.216 was added also to the Li for a better description of polarization.[10] Unrestricted Hartree−Fock (UHF) calculations were used throughout.

In solid state *ab initio* calculations, another factor besides the basis set selection that may influence the result is how, in principle, the infinite number of two-electron integrals are evaluated. In the *Crystal* program, Coulomb integrals between nonoverlapping charge distributions are evaluated by multipolar expansion and subsequent Ewald summation of the multipole series.[19] Where the overlap between charge distributions are sufficiently large, the integrals are evaluated exactly. Cutoff criteria determine the division between the different Coulomb integral calculation modes, other cutoff criteria decide the accuracy for which exchange integral series are evaluated. For the sake of reproducibility, we simply note that the cutoff parameters t_n, $n = 1, 5$ (which corresponds to the cutoff limits 10^{-tn}) used in the *Crystal* program were set to (8,8,8,8,16) in the equilibrium geometry calculations and to (6,6,6,7,14) in the transition state geometry calculations. These parameters also affect the amount of disk integral storage required, and the chosen values represent the maximum accuracy we could afford with our present available disk size resources (about 1.5 GBytes).

In the *Crystal* calculations, the unit cell symmetries $I\bar{4}m2$ (No. 119) and $Pmn2_1$ (No. 31) were used for the equilibrium and transition state structures, respectively. The crystal cell contains two titanium dioxide units and one alkali metal atom, corresponding to the formula Li_xTiO_2, where $x = 0.5$. Geometry optimizations were performed for the cell dimensions and all the ion coordinates not determined by symmetry for the equilibrium and transition state structures in the prescribed space group. Since the *Crystal* program does not calculate analytical gradients, it was necessary to use single-point energy calculations in the geometry optimization. Gradients were obtained numerically from energy computations at small displacements from the starting coordinates. These gradients were utilized in the Polak−Ribiere gradient optimization scheme[20] to obtain a new guess for the equilibrium coordinates. This procedure was repeated until required convergence was achieved.

Modified INDO Computational Scheme. A version of the intermediate neglect of differential overlap (INDO) method, modified for crystal calculations (the CLUSTERD computer code[21]), which has been found very useful in the treatment of the electronic and spatial structure of perfect and defective crystals, was used for the semiempirical calculations. This technique is based on molecular orbital (MO) theory and a specific parametrization scheme.[22,23] The INDO parameter set for a particular element is optimized to match the main experimental features of the studied crystal: electronic band structure, the effective charges on the atoms, and the structural parameters, as well as the basic properties of some selected test molecules, e.g., equilibrium distance between the atoms in the molecule and ionization potentials. The details of the TiO_2, rutile and anatase, parametrization are described in refs 3 and 24.

Two variants of the model have been used up to now in crystal studies: (i) the periodic large unit cell (LUC) model,[25] which calculates both the electronic structure and the total energy of the perfect crystal via MO as linear combinations of atomic orbitals (AO's) and (ii) the embedded molecular cluster (EMC) model,[26] which also is based on a strict treatment of the total energy of the whole crystal, accounting for the perturbation (polarization) that the remaining crystal has on the EMC region, thus leading to the so-called quantum cluster approach.

The LUC has been used mainly for the parametrization procedure of the perfect crystals, whereas the EMC model has been applied to investigate defective crystals. This is mainly because of the difficulties in avoiding the mutual perturbation of periodically arranged defects when the LUC model is applied. Despite these limitations of the LUC approach, some successful attempts have recently been done in applying the periodic model, e.g., study of charge and potential distribution near the (100) GaP surface,[27] investigation of triplet exciton self-trapping and Frenkel-defect pair creation in the a-SiO_2 crystal,[28] stability studies of hydrogen-doped Si, GaAs, and CdTe semiconductors,[29,30] and studies of bound hole polarons (V_{Mg} centers) in corundum crystals.[31] It has to be noted that the periodic LUC model considers the electronic band structure and calculates the total energy of the system more accurately than the EMC, due to not only the periodicity condition but also a careful treatment of exchange interaction, which is omitted in the EMC case between the EMC region and the residual part of the crystal. This was the reason why we chose the LUC model in the present study despite the fact that the EMC approach was utilized in our previous work[3] on TiO_2 crystals. In particular, using the LUC we improved considerably the self-consistent field (SCF) convergence near the transition state for the diffusion path and consequently the reliability of our results.

A full account of the method used to calculate the total energy of the crystal within the LUC framework is found in refs 21, 25, and 32. We will therefore restrict ourselves to the most important features of the LUC approach. The heart of the method consists of computing the electronic structure of the unit cell extended in a special manner at $\mathbf{k} = 0$ in the reduced Brillouin zone (BZ). This is equivalent to a band structure calculation at those BZ $\mathbf{k}$ points, which transform to the reduced BZ center on extending the unit cell. The total energy of the LUC is

$$E_{\mathrm{LUC}} = \frac{1}{2}\sum_{\mathrm{A}\neq\mathrm{B}}\frac{Z_{\mathrm{A}}Z_{\mathrm{B}}}{R^{00}_{\mathrm{AB}}} + \frac{1}{2}\sum_{\mathrm{A}\in\mathrm{LUC}} E^{\mathrm{A}}_{\mathrm{C}} + \sum_{j}^{N_{\mathrm{occ}}}\epsilon_j(0) + \frac{1}{2}\sum_{\mu,\nu\in\mathrm{LUC}}\rho_{\mu\nu}(0)Q_{\mu\nu} \quad (1)$$

Here, $\epsilon_j(\mathbf{k})$ are the eigenvalues of the Fock matrix, N_{occ} is the number

(10) Ojamäe, L.; Hermansson, K.; Pisani, C.; Causà M.; Roetti, C. *Acta Crystallogr. B* **1994**, *50*, 268.
(11) Silvi, B.; Fourati, N.; Nada, R.; Catlow, C. R. A. *J. Phys. Chem. Solids* **1991**, *52*, 1005.
(12) Reinhardt, P.; Hess, B. A.; Causà, M. *Int. J. Quantum Chem.* **1996**, *58*, 297.
(13) Fahmi, A.; Minot, C.; Silvi, B.; Causà, M. *Phys. Rev. B* **1993**, *47*, 11717.
(14) Orlando, R.; Azavant, P.; Towler, M. D.; Dovesi, R.; Roetti, C. *J. Phys.: Condens. Matter* **1996**, *8*, 1123.
(15) Mackrodt, W. C.; Harrison, N. M.; Saunders, V. R.; Allan, N. L.; Towler, M. D. *Chem. Phys. Lett.* **1996**, *250*, 66.
(16) Corà, F.; Patel, A.; Harrison, N. M.; Dovesi, R.; Catlow, C. R. A. *J. Am. Chem. Soc.* **1996**, *118*, 12174.
(17) Durand, P.; Barthelat, J. C. *Theor. Chim. Acta* **1975**, *38*, 283.
(18) Bouteiller, Y.; Mijoule, C.; Nizam, M.; Barthelat, J. C.; Daudey, J. P.; Pelissier M.; Silvi, B. *Mol. Phys.* **1988**, *65*, 295.
(19) Dovesi, R.; Pisani, C.; Roetti, C.; Saunders, V. R. *Phys. Rev. B* **1983**, *28*, 5784.
(20) Press, W. H.; Flannery, B. P.; Teukolsky, S. A.; Vetterling, W. T. *Numerical Recipes*; Cambridge Univiversity Press: New York, 1986.
(21) Stefanovich, E. V.; Shidlovskaya, E. K.; Shluger, A. L.; Zakharov, M. A. *Phys. Status Solidi B* **1990**, *160*, 529.
(22) Pople, J.; Beveridge, D. *Approximate MO Theories*; McGraw-Hill: New York, 1970.
(23) Shluger, A. *Theor. Chim. Acta* **1985**, *66*, 355.
(24) Stashans, A.; Lunell, S.; Grimes, R. W. *J. Phys. Chem. Solids* **1996**, *57*, 1293.
(25) Evarestov, R. A.; Lovchikov, V. A. *Phys. Status Solidi B* **1977**, *79*, 743.
(26) Kantorovich, L. N. *J. Phys. C* **1988**, *29*, 5041.
(27) Stefanovich, E. V.; Shluger, A. L. *J. Phys.: Condens. Matter* **1994**, *6*, 4255.
(28) Shluger, A.; Stefanovich, E. *Phys. Rev. B* **1990**, *42*, 9664.
(29) Stashans, A.; Kitamura, M. *Solid State Commun.* **1996**, *99*, 583.
(30) Stashans, A.; Kitamura, M. *J. Phys. Chem. Solids*, in press.
(31) Zhukovskii, Yu. F.; Kotomin, E. A.; Nieminen, R. M.; Devreese, J. T.; Stashans, A. In *Optical Inorganic Dielectric Materials and Devices*, SPIE Proc., Vol. 2967; SPIE: Bellingham, WA, 1997; p 153.
(32) Smith, P. V.; Szymanski, J. E.; Matthew, J. A. D. *J. Phys. C* **1985**, *18*, 3157.

of occupied electronic states in the system, $\rho_{\mu\nu}(\mathbf{k})$ are the density-matrix elements in the basis of the Bloch orbitals, and

$$E^{A}{}_{C} = Z_A \sum_{l\neq 0} \sum_{B\in LUC} \left[\frac{Z_B}{R^{0l}_{AB}} - \sum_{\mu\in B} \rho_{\mu\mu}(0)(v^{A0})^{ll}_{\mu\mu} \right] \quad (2)$$

$$Q_{\mu\nu} = T^{00}_{\mu\mu} - \sum_{A\in LUC} Z_A (v^{A0})^{00}_{\mu\mu} + \sum_{l\neq 0} H^{01}_{\mu\mu}, \quad \text{if } \mu = \nu \quad (3)$$

$$Q_{\mu\nu} = \sum_{l} H^{0l}_{\mu\nu}, \quad \text{if } \mu \neq \nu \quad (4)$$

where $T^{00}_{\mu\mu}$ are the matrix elements of the kinetic-energy operator, $(v^{A0})_{\mu\mu}$ are those of the electron-core interaction operator, R^{01}_{AB} is the distance between the cores of atoms A and B, and Z_A and Z_B are the charges of these cores. The Coulomb interaction is treated quite well in the LUC model, thanks to the theory of special **k** points.[33] The Coulomb lattice sums are calculated using Ewald's method,[34] which was generalized to the case of an arbitrary lattice.[35] The exchange interaction is computed after introducing the cutoff function,[32]

$$\omega(r_{\mu\nu}) \equiv \frac{P^{01}_{\mu\nu}}{\rho_{\mu\nu}(0)} \quad (5)$$

where $P^{0l}_{\mu\nu}$ is the density matrix in the AO basis and $r_{\mu\nu}$ is the interatomic distance. However, as was shown in ref 21, $P^{0l}_{\mu\nu}$ should be close to zero when $r_{\mu\nu}$ is larger than $R_c/2$, where R_c is the characteristic length of the translational vector of the LUC used. This requirement can be fulfilled by considering larger LUC.

In our case, a periodic 48-atom LUC (supercell) was considered to study Li and Na diffusion, i.e., we used an 8-fold-symmetric extension of the anatase primitive unit cell. The first attempt to study theoretically cation diffusion in anatase using the same size supercell was done in ref 5. As indicated by numerous computations,[21,28,33] an 8-fold- or even 4-fold-symmetric extension of the primitive unit cell proves to be completely sufficient for a correct reproduction of the electronic density distribution in the crystal. The problem of avoiding the mutual perturbation of periodically arranged impurities did not arise in our case because the impurity concentration corresponds to the experimentally verified values.[3]

Experimental Method

To experimentally determine the activation energies, chronocoloumetry was applied. Briefly, in these experiments the electrode is perturbed by applying a sufficiently large potential step to the electrode. By following the time evolution of the integrated charge transport currents, information about the diffusion processes can be obtained.

Electrodes. The electrode preparation followed the procedure described by Kurtz and Gordon.[36] Thin films were chemically vapor deposited onto a conducting glass substrate (F-doped SnO_2, 8 Ω/square). A mixture of tetrakis(isopropyloxy)titanium $[Ti(OiPr)]_4$ and niobium ethoxide was used as precursor. Argon was used as carrier gas (flow speed: 4.2 L min^{-1}). The niobium content in the electrodes was 1, 2, and 5 atomic percents. The deposition temperature was 450 °C. All electrodes were postannealed in a stream of hot air at 450 °C for 30 min and transferred directly to the electrochemical cell in a desiccator. The structure characterization was performed by a Siemens D-5000 diffractometer, showing that all samples consisted of anatase.

(33) Evarestov, R. A. *Quantum-Chemical Methods in Solid State Theory*; Leningrad State University Press: Leningrad, 1982.

(34) Born, M.; Huang, K. *Dynamic Theory of Crystal Lattices*; Oxford University Press: London, 1954.

(35) Shidlovskaya, E. K.; Stefanovich, E. V.; Shluger, A. L. *Russian J. Phys. Chem.* **1988**, *62*, 1352.

(36) Kurtz, S. R.; Gordon, R. G. *Thin Solid Films* **1987**, *147*, 167.

Table 1. Geometry-Optimized Unit Cells of Pure Anatase[8] and of Anatase Containing Alkali-Metal Ion Defects Obtained from the *ab Initio* Calculations[a]

structure	TiO_2 (ref 13)	$Li_{0.5}TiO_2$	$Na_{0.5}TiO_2$
a (Å)	3.763	3.962	4.076
c (Å)	9.851	9.604	9.444
Ti_I *x*, *y*, *z*	0, 0, 0	0, 0, 0	0, 0, 0
Ti_{II} *x*, *y*, *z*	0, 0.5, 0.25	0, 0.5, 0.25	0, 0.5, 0.25
O_I *x*, *y*, *z*	0, 0.5, 0.0475	0, 0.5, 0.0465	0, 0.5, 0.0480
O_{II} *x*, *y*, *z*	0, 0, 0.2025	0, 0, 0.2171	0, 0, 0.2184
Li/Na *x*, *y*, *z*		0.5, 0.5, 0.0	0.5, 0.5, 0.0

[a] The space group is $I\bar{4}m2$. Cell dimensions and positions not defined by symmetry were optimized.

Electrolyte. The electrolyte consisted of 1 M $LiCF_3SO_3$ and 1 M $NaClO_4$ (Aldrich) in acetonitrile (Aldrich). The salts were vacuum-dried at 140 °C ($LiCF_3SO_3$) and 200 °C ($NaClO_4$) for 48 h. The solvent contained less than 50 ppm water (as received) and was further dried for several weeks over activated molecular sieves before it was mixed with the salts. The electrolyte solutions were stored in Sure Seal bottles (Aldrich) under an Ar atmosphere. All chemicals used were of reagent grade.

Electrochemical Measurements. The electrochemistry was performed using a three-electrode system connected to a multichannel ECO Chemie Autolab/GPES electrochemical interface. For the electrochemistry a thermostatically controlled Metrohm glass vessel was used. The vessel was dried overnight at 110 °C and purged for several hours with dried Ar together with the mounted electrodes before the electrolyte was added. Electrolyte (100 mL) was injected into the chamber using Omnifit Teflon tubings with connections for chromatography. The counter electrode consisted of glassy carbon and was enclosed with a glass frit to avoid the influence of reaction products. The reference was Ag/AgCl in saturated LiCl (Merck) in anhydrous acetonitrile. The LiCl was dried at 200 °C for several weeks before use. All potentials are referred to the Ag/AgCl electrode. The potential variation of the reference electrode between 25 and 60 °C was less than 3 mV. The atmosphere in the cell compartment was purged with a slight overpressure of Ar. The initial water content from the Ar tube was less than 5 ppm, and the gas was predried in a glass column (40 cm) containing activated molecular sieves (4 Å), before the inlet to the cell compartment. To avoid the build up of a diffusion layer outside the TiO_2 films, the electrolyte solution was heavily stirred with a magnetic stirrer during all experiments. A Pt electrode was used in situ as an indicator of the relative water content. By cycling the Pt electrode between 0 and −1.5 V at 20 mV s^{-1}, a very small residual current (mainly capacitive, no redox peaks) of ∼10 μA/cm^2 was observed. All potential steps were performed after the electrode was kept at a potential of 0 V for 30 min.

Results and Discussion

Theoretical Section. Equilibrium Structures. The structure of anatase has the tetragonal body-centered space group $I4_1/amd$ (D^{19}_{4h}) with a crystallographic unit consisting of two unit cells, i.e., four molecular units. In this arrangement the distances between a titanium and its six octahedrally coordinated oxygens are nearly equal while the oxygen octahedron is not regular. The structure of the pure TiO_2 anatase phase using the *Crystal* program has been studied by Fahmi *et al.*,[13] where they calculated the geometry-optimized structure using the same basis set as that used for TiO_2 in the present *ab initio* study. Their results for the structure are listed in Table 1. The structural parameters within the INDO method (a = 3.69 Å, c

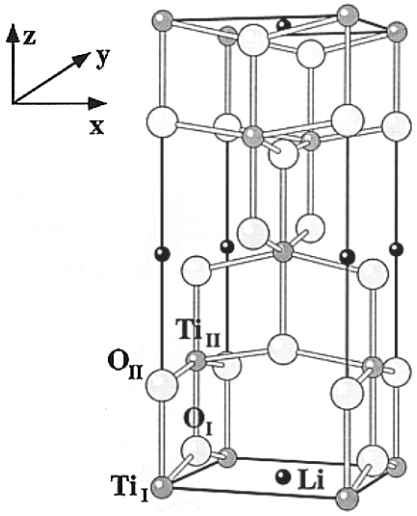

Figure 1. The unit cell of $Li_{0.5}TiO_2$ obtained from the *ab initio* geometry optimization: black ions, Li; gray ions, Ti; white ions, O. The space group is $I\bar{4}m2$.

= 10.07 Å, $u = 0.20$) have been optimized in ref 24 and are used in the present INDO investigation. They are close to the experimental constants:[37] $a = 3.784$ Å, $c = 9.515$ Å, and $u = 0.208$.

When an alkali metal ion is dissolved in the structure, the symmetry of the unit cell decreases from the original $I4_1/amd$ to the $I\bar{4}m2$ space group symmetry. Calculation of the lattice energy for different displacements of Li along the *z*- and *x*-coordinates gave as a result that the equilibrium position of the alkali metal ion has the coordinates (0.5, 0.5, 0), which is an octahedral interstitial site. (The reason for choosing these particular subgroups is that for the sake of computational efficiency at least one of the mirror planes should be conserved.) Since there is one alkali metal ion per unit cell, this corresponds to half of the octahedral interstitial sites being occupied. The two titaniums are no longer equivalent in the inclusion compound, nor are the two oxygens. Our *ab initio* results from geometry optimization of the alkali-metal-containing structures can be also seen in Table 1. The structure of $Li_{0.5}TiO_2$ is displayed in Figure 1.

Compared to the pure phase, the *a*-axis increases by 0.20 Å and the *c*-axis decreases by 0.25 Å in the Li-containing compound, whereas for the Na compound the increase and decrease are 0.31 and 0.41 Å, respectively (see Table 1).

The effect of the alkali metal ion inclusion is to increase the distance between the Ti ion and the four nearest oxygens approximately in the *xy*-plane, the "equatorial" oxygens. The distance between titanium and the oxygens along the z-axis, the "axial" oxygens, *decreases* upon ion inclusion for the Ti ion closest to the alkali metal ion, but *increases* for the Ti ion situated in the second non-equivalent position (Ti_{II}), see Table 2. If Li and Na inclusion is compared, it is interesting to note that the $Ti-O_{eq}$ distances are larger for Na than for Li, but the $Ti-O_{ax}$ distance remains constant or smaller for Na than for Li (which is also reflected directly in the variation of cell-axis lengths, see Table 1). The distance between the equatorial oxygen and the alkali metal ion is similarly longer for Na than for Li, but shorter for the axial oxygen.

The INDO calculations show that the impurity finds itself located not exactly in the interstitial octahedral site but slightly distorted toward one of the Ti ions, which receives an unpaired electron. This very small distortion, ~0.06 Å, is required to reduce the symmetry, so that the electron density is located mainly on *one* titanium—that closest to the impurity. If the impurity ion is situated exactly in the interstitial octahedral site, the electron is shared equally by the *four* closest titaniums, and this is not a stable position for the impurity, as predicted by the INDO computations. The results of the crystalline framework distortion, obtained by automated geometry optimization procedure, are shown in Table 3. Titaniums move outward from the impurity due to the electron overlap repulsion and electrostatic Coulomb repulsion mechanisms, thus allowing the alkali-metal ion to jump more easily from one equilibrium position to another. The displacements of the oxygens are more complex because of the following reasons: (i) O ions tend to move away from the impurity due to the repulsion occuring as a result of electron overlap, (ii) they tend to move toward the impurity since they have opposite effective charges, and, finally, (iii) oxygens try to adjust to the displacements of the nearest Ti ions due to the strong bonding between Ti and O. Only the distortions for the four Ti ions and six O ions closest to the impurity were found to be non-negligible and are displayed in Table 3.

(37) Abrahams, S. C.; Bernstein, J. L. *J. Chem. Phys.* **1971**, *55*, 3206.

Table 2. Interatomic Distances in the Geometry-Optimized Equilibrium Structures (Å) from *ab Initio* Calculations[a]

structure	TiO_2 (ref 8)	$Li_{0.5}TiO_2$	$Na_{0.5}TiO_2$
Ti_I-O_{eq}	1.94	2.03	2.06
$Ti_{II}-O_{eq}$	1.94	2.01	2.06
Ti_I-O_{ax}	1.99	2.09	2.09
$Ti_{II}-O_{ax}$	1.99	1.95	1.91
$Me-O_{eq}$		2.03	2.09
$Me-O_{ax}$		2.72	2.66
$Me-Ti_I$		2.80	2.88
$Me-Ti_{II}$		3.11	3.12

[a] O_{eq} denotes the nearest oxygen which is situated approximately in the same *xy*-plane as the Ti ion, e.g., Ti_I-O_I. O_{ax} denotes the nearest oxygen along the *z*-axis relative the Ti ion, e.g., Ti_I-O_{II}. Me denotes Li or Na.

Table 3. Lattice Distortions (Å) for the Equilibrium and Transition State Geometries for Li and Na Diffusion in TiO_2 Anatase from INDO Calculations[a]

	equilibrium state		transition state	
atom	Li impurity	Na impurity	Li impurity	Na impurity
titaniums	0.03−0.07	0.03−0.10	0.04−0.08	0.04−0.13
oxygens	0.03−0.08	0.04−0.10	0.04−0.10	0.04−0.11

[a] The absolute values of the distortions for the four impurity-closest Ti atoms and six impurity-closest O atoms are indicated for the case of $Me_{0.0625}TiO_2$.

Transition Structures. The diffusion of the alkali metal ions in the anatase framework will occur along a reaction path connecting the octahedral vacant interstitial sites. A transition-state structure of the ion diffusion was identified from symmetry considerations (and from potential-energy calculations on a linear path connecting two octahedral interstitial sites at (0.5, 0.5, 0) and (0.5, 0, 0.25)) to be situated at, or in close vicinity of, the position (0.5, 0.25, 0.125). At this point the diffusing ion is equidistant to four Ti ions: two Ti_I ions along the *x*-axis and two Ti_{II} ions in a line parallel to the *x*-axis. The diffusion path is shown schematically in Figure 2.

In our *ab initio* computations the structure at the transition state point was geometry-optimized, by requiring the diffusing ion to remain equidistant to the four Ti ions. The space group symmetry was reduced to the orthorombic $Pmn2_1$ (No. 31) due to the loss of symmetry along the *y*-direction. The structural parameters of the optimized transition−state structures can be seen in Table 4. At the transition state geometry Li is quite close to the two oxygens at distances 1.81 and 1.94 Å. For Na

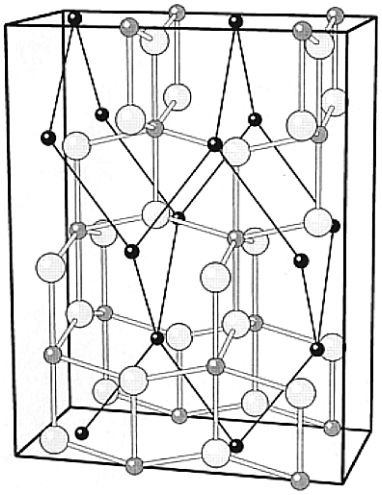

Figure 2. Schematic diagram displaying the diffusion paths. Octahedral interstitial sites are represented by the black ions. The transition state is situated at the midpoint connecting the octahedral interstitial sites. The cell shown is twice the unit cell in the *y*-direction in the space group $Pmn2_1$.

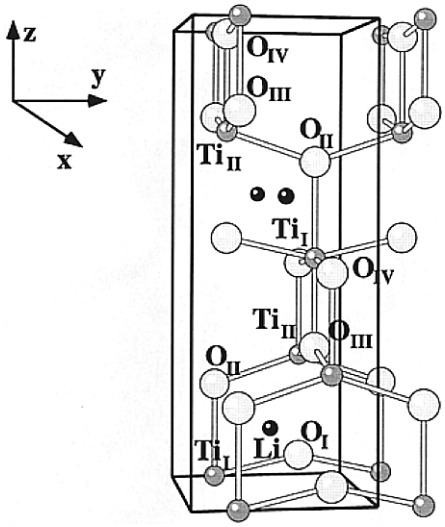

Figure 3. The optimized unit cell for the transition state structure of $Li_{0.5}TiO_2$. The Li ion is situated at equal distances from four Ti ions. The cell shown is the unit cell in the space group $Pmn2_1$, which is related to the $I\bar{4}m2$ unit cell through a translation of 0.25 in the *y*-direction.

Table 4. Geometry-Optimized Unit Cells of the Transition State Structures from *ab Initio* Calculations[a]

structure	$Li_{0.5}TiO_2$	$Na_{0.5}TiO_2$
a (Å)	4.093	4.124
b (Å)	3.778	3.668
c (Å)	9.861	10.607
Ti_I *x*, *y*, *z*	0, 0.25, 0	0, 0.25, 0
Ti_{II} *x*, *y*, *z*	0, 0.75, 0.2712	0, 0.75, 0.2853
O_I *x*, *y*, *z*	0, 0.75, 0.0434	0, 0.75, 0.0482
O_{II} *x*, *y*, *z*	0, 0.25, 0.2071	0, 0.25, 0.2134
O_{III} *x*, *y*, *z*	0, 0.25, 0.8075	0, 0.25, 0.8257
O_{IV} *x*, *y*, *z*	0, 0.75, 0.4793	0, 0.75, 0.4745
Li/Na *x*, *y*, *z*	0, 0.50, 0.1356	0, 0.50, 0.1427

[a] The space group is $Pmn2_1$. Diffusion is assumed to occur parallel to the *y*-axis from the position (0.5, 0.75, 0) to the position (0.5, 0.25, 0.25) in this space group (note the translation of $y = 0.25$ compared to the $I\bar{4}m2$ unit cell).

the corresponding distances are 2.01 and 2.15 Å. The distances to the four titanium ions are 2.62 Å in the case of Li and 2.72 Å in the Na case.

Table 5. Alkali-Metal Ion Diffusion Barrier Heights (eV) in TiO_2 Anatase[a]

	theory		experiment	
	ab initio	INDO	ref 5	this paper
Li_xTiO_2			0.51, 0.66	0.6 ± 0.1
$x = 0.0625$		0.51		
$x = 0.25$		0.54		
$x = 0.5$	0.60	0.56		
Na_xTiO_2			1.60, 1.78	0.52 ± 0.1
$x = 0.0625$		0.54		
$x = 0.25$		0.55		
$x = 0.5$	0.55	0.56		

[a] The two experimental values from ref 5 correspond to $x < 0.5$ and $x > 0.5$ for Me_xTiO_2, respectively.

In our INDO computations we did not need to assume *a priori* any requirements on the diffusing ion geometry or the way of relaxation for the vicinity ions. Still, the minimal-energy configuration for an impurity was found to be practically in (0.5, 0.25, 0.125), i.e., the same as in the *ab initio* calculations. The relaxation of vicinity ions in the case when the impurity resides in the transition state is only slightly larger (see Table 3) compared to the geometry relaxation of the equilibrium state. However, the gain in relaxation energy for the transition state exceeds the corresponding value for the equilibrium state, thus reducing the activation energy. The length of the diffusion path is 3.11 Å, assuming the INDO structural parameters, or 3.04 Å if we consider the experimental values of structural parameters for the anatase. We should point out that we have only found one kind of diffusion path in anatase, i.e. there is only one kind of transition state. The transition state T_I mentioned in our previous report[5] was not confirmed by the *ab initio* computations of the present study. We can assume that this state is a local minimum on the total energy surface for two reasons: (i) the obtained values for activation energies for this state are unexpectedly small and (ii) it is located too close to the one of the equilibrium states (see ref 5 for more details).

One can notice (see Table 3) the similar lattice relaxations, independent of the kind of impurity, Li or Na. The radius[38] of the Na ion, 1.02 Å, is larger that of the Li ion, 0.76 Å, but apparently Li^+ has excessive binding energy and additionally is less polarizable than the Na ion, explaining why the Na^+ causes similar distortions for the vicinity ions as the Li^+ does despite its larger size.

Charge Distributions. The electron density analysis, carried out by both theoretical methods, gives the following pattern. In the equilibrium structures, the atomic charges according to a Mulliken population analysis in the *ab initio* approach are +0.79 e for Li and +0.99 e for Na. An almost complete ionization of the inclusion ions has thus occurred. An analysis of the spin density reveals that an electron transfer has occurred from the alkali metal impurity to the Ti ion. The unpaired electron is occupying one of the empty d-orbitals of the Ti_I ion. The semiempirical calculations, using Löwdin population analysis, give the following values for atomic charges of impurity: +0.82 e and +0.96 e for Li and Na, respectively.

At the transition state, the Mulliken charges on Li and Na are +0.77 e and +0.94 e, respectively (*ab initio*), and the Löwdin charges on Li and Na are +0.81 e and +0.95 e, respectively (INDO). They are similar to the charges at the equilibrium position. Also in the transition state case, the extra spin is found on one of the Ti ions. A difference is however that the electron is in a d-orbital on a Ti_{II} ion instead of on Ti_I. The electron thus switches its location from one ion to another

(38) *Handbook of Chemistry and Physics*; Lide, D. R., Ed.; CRC Press: Boca Raton, FL, 1992.

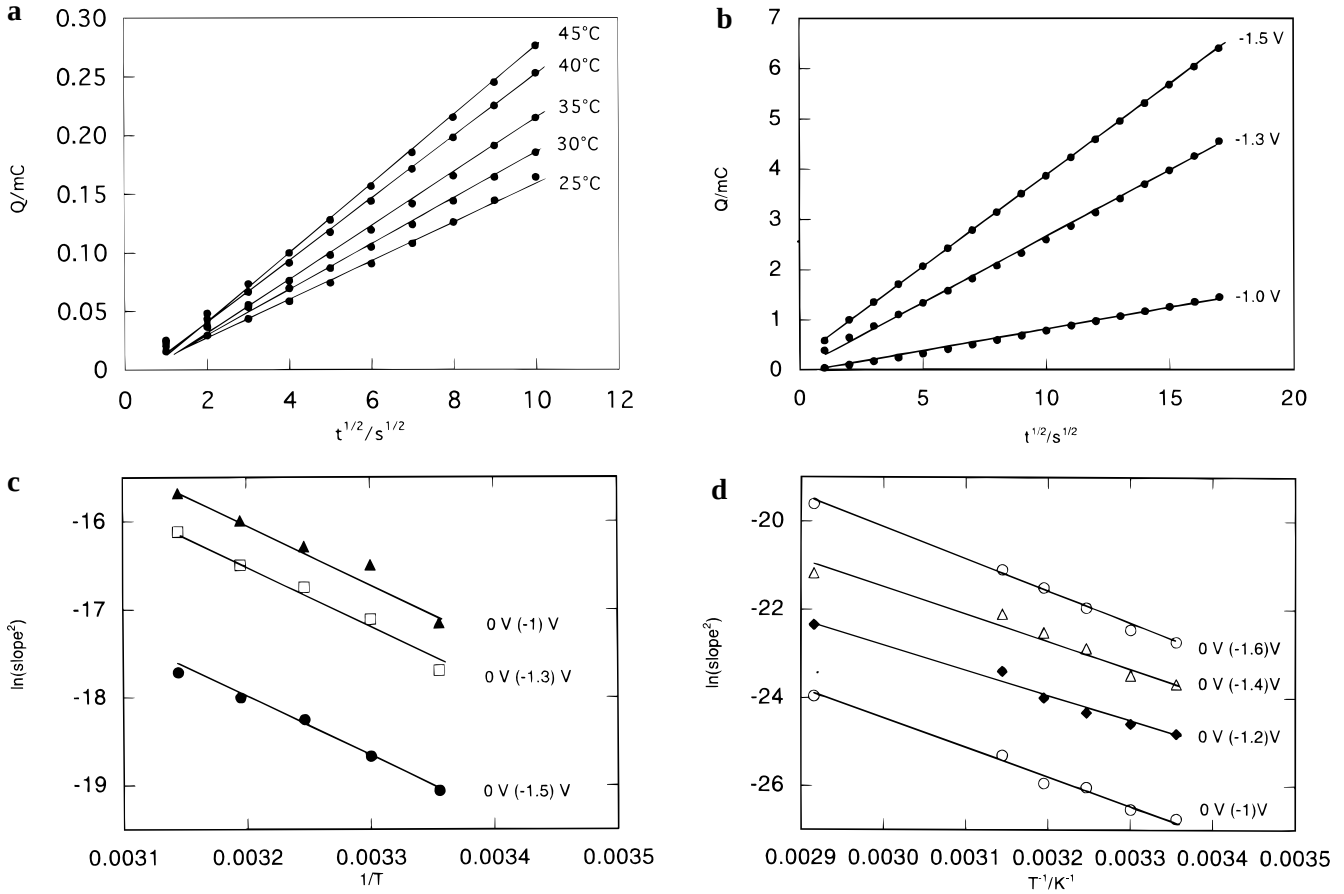

Figure 4. (a) The integrated charge vs $t^{1/2}$ at different temperatures for Na^+ insertion. The potential step was made from 0 to −1.4 V. (b) The integrated charge vs $t^{1/2}$ at different potential steps for Li^+ insertion. The temperature was 45 °C. (c) The logarithm of the slope from Q vs $t^{1/2}$ plots vs the inverse temperature for Li^+ insertion. (d) The logarithm of the slope from Q vs $t^{1/2}$ plots vs the inverse temperature for Na^+ insertion. The niobium content was in all cases 1 atomic percent.

during the diffusion process. A tentative picture might be that the electron moves during the diffusion process somewhat like a dog on a leash, tagging along its master, the alkali metal ion, but happily running to-and-from and sniffing on each titanium lamp post along the way.

Energy Barriers. In the *ab initio* computations, if the energy of the equilibrium structure was calculated using the *Crystal* cutoff parameters (8,8,8,8,16) and the energy of the transition state structure using the parameters (6,6,6,7,14), we obtained a Li diffusion barrier equal to 0.66 eV and a Na diffusion barrier equal to 0.60 eV. But since choosing different cutoff parameters implies different methods of integral calculation, spurious effects might be introduced by doing so. We therefore used the same cutoff parameters (6,6,6,7,14) for both states in a second calculation of the barrier. By doing this, we instead obtain a barrier equal to 0.60 eV for Li and 0.55 eV for Na, respectively.

The corresponding activation energy was calculated for several different impurity concentrations using the INDO method. We intercalated one, four, and eight impurities into the 48-atom anatase supercell, corresponding to cation/Ti ratios of 0.0625, 0.25, and 0.5, respectively. The calculated activation energies are given in Table 5. As one can see, no significant dependence of the energies upon the impurity concentration was observed. Moreover, for $x = 0.5$, the INDO values were very close to the *ab initio* ones, namely 0.56 eV for Li and 0.56 eV for Na. We can also note that the values of the lattice relaxation for $x = 0.25$ and $x = 0.5$ in Me_xTiO_2 are larger than those for $x = 0.0625$ (given in Table 3) by 12% and 20%, respectively.

Experimental Section

Theory. The measurements reported here aim at the activation energy, E_a, for Li and Na ion diffusion in anatase. The activation energy, E_a, may be determined by the following relationship

$$D = D_0 e^{-E_a/kT} \tag{6}$$

where D is the diffusion coefficient, D_0 is the pre-exponential factor, k is the Boltzmann constant, and T is the absolute temperature. Thus, a plot of ln D vs the inverse temperature gives the activation energy, E_a. The diffusion coefficient D can be determined from:[39]

$$Q = 2n\pi^{-1/2}FAD^{1/2}C^*t^{1/2} \tag{7}$$

describing the coloumetric response after a potential step at a planar electrode. Q is the integrated charge, A is the electroactive electrode area, D is the diffusion coefficient[40,41] and C^* is the surface concentration. Hence, plots of Q vs $t^{1/2}$ at different temperatures yield the desired parameters in eq 6. Note that in order to determine E_a in eq 6, it is not necessary to know the absolute value of D. Consequently, we need to determine simply the slope from a Q vs $t^{1/2}$ plot, which relates directly to D.

Measurements. Q vs $t^{1/2}$ plots for Na ion insertion at different temperatures are displayed in Figure 4a. The potential step was made from 0 to −1.4 V. It can be seen that the charge is directly proportional to the square root of the time and thus eq 7 is applicable. The increase

(39) Bard, A. J.; Faulkner, L. R. *Electrochemical Methods: Fundamentals and Applications*; John Wiley & Sons: New York, 1980.

(40) The chemical diffusion coefficient is obtained if only the concentration is considered, i.e., the activity gradient is not taken into account. See also ref 35.

(41) Weppner, W.; Huggins, R. A. *J. Electrochem. Soc.* **1977**, *124*, 1569.

of the integrated charge at higher temperatures shows that the diffusion process of Na^+ in the anatase lattice is thermally activated, i.e., the diffusion constant D is a function of temperature. The same feature was also observed for Li^+ ion insertion. Figure 4b displays typical Q vs $t^{1/2}$ plots for Li^+ insertion at different negative potential steps. The initial potential was 0 V. The increase of the slopes at more negative potential steps suggests, according to eq 7, that the surface concentration C^* is potential dependent, i.e., higher surface concentrations are obtained at more negative potentials. A similar potential dependence on the slope was also observed for the insertion of Na^+. Thus, it is possible to change the concentration gradient of Li^+ or Na^+ by changing the magnitude of the potential step.

Activation Energy. The activation energies for Li^+ and Na^+ diffusion were determined by plotting the logarithm of the slopes vs the inverse temperature as shown in Figures 4c,d. It can be seen that the activation energy for Li^+ diffusion decreases slightly at more negative potential steps, going from 0.7 eV (0 to −1 V) to 0.5 eV (0 to −1.5 V). However, for Na^+ diffusion all activation energies are scattered randomly around 0.5 eV, giving an average value of 0.52 eV (12 measurements). The obtained experimental activation energies thus agree well with those obtained from the calculations above both for Li and Na. We can note that the amount of niobium in the anatase (1−5 atomic percents) has no effect on the activation energy or the diffusion constant for Li^+ and Na^+ diffusion.

In the previous study[5] the activation energies for lithium and sodium diffusion were determined from impedance measurements on fluorinated titanium dioxide. The samples were produced by sputtering from a Ti target in the presence of O_2 and CF_4 and were amorphous according to X-ray diffraction. The obtained activation energies for lithium diffusion were 0.5−0.7 eV, in agreement with the present study. However, the activation energies for sodium diffusion, 1.6−1.8 eV, differed remarkably from the presently obtained value (0.52 eV). At present, the reasons for this discrepancy are unclear.

Conclusions

We have presented a study of Li and Na diffusion in TiO_2 anatase using two different theoretical methods supported by electrochemical experiments. The theoretical approach of applying both *ab initio* and INDO semiempirical calculations to study the same system is appealing, since whereas the *ab initio* results are precise, the semiempirical calculations allow us to study larger cells and thus investigate the importance of concentration and local-defect approximation.

The predictions of the *ab initio* and INDO calculations are very similar for both equilibrium and transition state configurations as well as the diffusion paths. The Li and Na ions are accommodated in the octahedral empty interstitial sites while the unpaired electron transfers to one of the closest titaniums. The diffusion of the alkali-metal ion occurs along a reaction path connecting the octahedral interstitial sites with a jump length of 3.04 Å.

The calculated activation energies for Li and Na ions by the *ab initio* and INDO methods agree remarkably well. Likewise, the agreement of either theoretical method with the present electrochemical experiments is very satisfactory for both types of impurities. However, there is a discrepancy for Na with earlier experimental work[5] (see also Table 5), where the chemical diffusion coefficients were obtained from impedance spectroscopy.

It is interesting to note that, although the Na ion has a noticeably larger radius that the Li ion, its barrier toward diffusion is not larger. The present results thus indicate that the classical ionic radius of the diffusing ion plays a less dominant role than its ability to polarize its surroundings.

Acknowledgment. This work was supported by the Swedish Research Council for Engineering Sciences (TFR), the Swedish Natural Science Research Council (NFR), the Swedish National Supercomputer Centre (NSC), and the European Community Joule III program.

JA9708629